LAWRENCE
LIVERMORE
NATIONAL
LABORATORY

UCRL-JRNL-226260

Ion Deflection for Final Optics In Laser Inertial Fusion Power Plants

R. P. Abbott, J. F. Latkowski

November 21, 2006

Fusion Science and Technology

ION DEFLECTION FOR FINAL OPTICS IN LASER INERTIAL FUSION POWER PLANTS

Ryan P. Abbott and Jeffery F. Latkowski

Lawrence Livermore National Laboratory, 7000 East Avenue, Livermore, CA, 94550, abbott13@llnl.gov

Left unprotected, both transmissive and reflective final optics in a laser inertial fusion power plant would quickly fail from melting, pulsed thermal stresses, or degradation of optical properties as a result of ion implantation. One potential option for mitigating this threat is to magnetically deflect the ions such that they are directed into a robust energy dump. In this paper we detail integrated studies that have been carried out to asses the viability of this approach for protecting final optics.

I. INTRODUCTION

Inertial confinement fusion (ICF) is a process that can be initiated by forcing targets containing deuterium and tritium (DT) to states of high density and temperature using heavy-ion, pulsed power, or laser drivers. A sufficiently powerful driver coupled to properly designed targets can yield significantly more energy than is needed to initiate these fusion reactions. This has motivated various designs for power plants based on the harnessing of inertial fusion energy (IFE).[1,2,3]

The SOMBRERO point design advocated a krypton fluoride (KrF) laser driver while more recent progress in the development of the diode-pumped solid-state laser (DPSSL) under the High Average Power Laser (HAPL) program has helped make it a viable option as well.[4,5] Both laser types could employ grazing incidence metal mirrors (GIMMs) made from aluminum as final optics, but the DPSSL also has the option of using a transmissive Fresnel optic made from silica.[6]

Both transmissive and reflective final optics would face performance and survivability threats from the three types of energetic particles produced in the DT fusion reactions: photons, neutrons, and ions. The SOMBRERO design addressed the threat from ions by calling for a xenon background gas in the target chamber at a density of 1.8×10^{22} m^{-3}. At this density the ions would slow in and heat the xenon which would then re-radiate x-rays to the first-wall and final optics over a considerably lengthened period of time. The benefit of this would be to reduce the temperature spikes and thermal stresses on these components to acceptable levels.[7]

As the cryogenic targets need to be kept below the DT fuel's triple point temperature so that a stable implosion to be achieved, target heating during injection and transit through the chamber was considered. The SOMBRERO report concluded that while the target would experience a convective heat flux from the xenon gas of 4.2×10^{4} W/m^2, this would be dominated by the irradiative heating of 5.4×10^{5} W/m^2 from exposure to the infrared (IR) radiation given off by the hot first-wall at 1758 K. It was estimated that the target's polystyrene surface would rise to 700 K by the time it reached the center of a 6.5 m radius chamber when injected at 150 m/s.[8] This was identified as an area for further study.

Unfortunately, while more recent target design calculations have shown that the IR heating can be reduced by 96% with the addition of a reflective high-Z (currently gold and palladium) outer layer, xenon condensing on the target during injection has been identified as a heating mechanism far superior to the convective model considered in the SOMBRERO report and is now viewed as the greatest thermal challenge facing the design of survivable targets. And while the robustness of capsules could be significantly improved by addition of an insulating foam layer, background xenon gas densities will still have to be reduced by a factor of ten to fifty from those called for in the SOMBRERO design.[9] Some have even advocated its elimination altogether in favor of vacuum. This constraint has had a significant impact on several aspects of the chamber design with one of the most critical being the survival of the final optics.

With a background xenon density of 1.6×10^{22} m^{-3} (0.5 Torr at 300 K) a surface 26 m from chamber center could expect to see a ^{4}He ion fluence of 8.1×10^{14} m^{-2} per shot with an average energy of 220 keV from the standard 350 MJ HAPL direct drive target. If this density must be reduced fifty fold, the fluence increases to 1.9×10^{16} m^{-2} per shot with an average ion energy of 4.3 MeV. Bubble and blister formation is well documented in aluminum

irradiated at fluences as little as 5×10^{21} m^{-2}.[10] This corresponds to just 7 days for a GIMM inclined at 85° in an IFE power plant running at a frequency of 5 Hz.

Moreover, calculations modeling the ion deposition in a GIMM under these conditions indicate that the compressive stresses produced by ion heating could force its surface into plastic compression and pose a severe cracking threat. The relatively low thermal conductivity of SiO_2 leads to a bleaker story for Fresnel final optics. Similar calculations indicate that their surfaces will reach silica's melting temperature of 2100 K every shot.[11]

One possibility for reducing or eliminating the threats to final optics from ion irradiation would be to magnetically deflect them into robust energy dumps such as the beam tube walls. Fig. 1 illustrates this concept showing a gas filled target chamber and laser beam tube along with a field generated by a pair of dipole magnets. Also depicted are three possible resulting ion trajectories. The first shows the path of an ion stopped by the background gas, the second shows a deflected ion that still manages to reach the final optic, and the third shows a successfully perturbed ion impacting the beam tube.

This paper details integrated calculations showing that a system like shown in Fig. 1 can protect each of the 60 (48 for a power plant using Fresnels) final optics in a laser IFE power plant. We demonstrate that modest fields which can be generated using normally conducting electromagnetic coils are sufficient to drastically reduce the ion fluence on the final optics. Estimates of how much power these systems will require are provided and show that this solution can be implemented with reasonable impact an IFE plant.

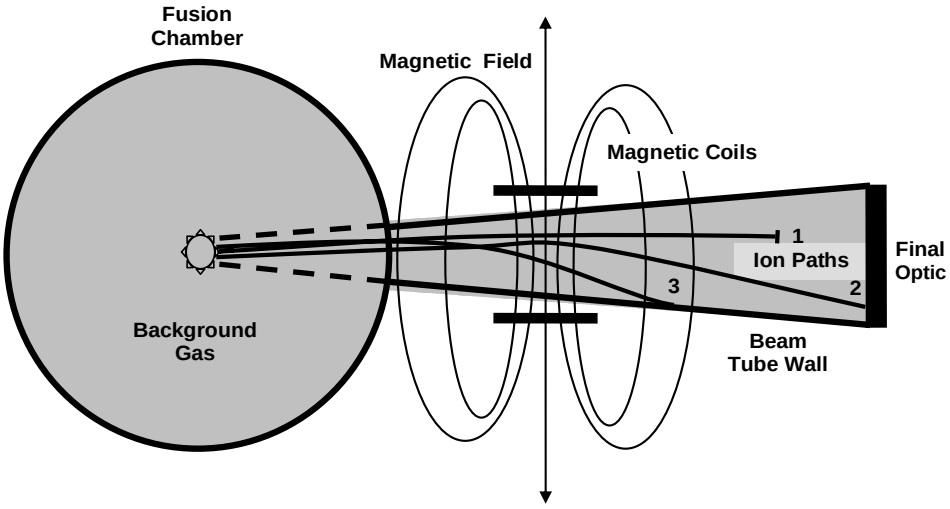

Fig. 1. A depiction of the ion mitigation concept showing three possible ion paths: (1) stopped by the background gas, (2) an optic intercepting path, and (3) a path where an ion is successfully deflected into the beam tube wall.

II. ION TRANSPORT MODELING

A code called Deflector was written to allow evaluation of the effectiveness of the magnetic deflection scheme depicted in Fig. 1. It can be setup to simulate what will happen for a variety possible final optic and chamber configurations, magnetic coil parameters, and background gas conditions. It takes in user specified chamber geometry, magnetic field profile, background gas conditions, and ion spectra data and proceeds to determine the paths the ions will follow from their birth at chamber center to their ultimate positions either stopped in the background gas or impacting the beam tube wall or final optic. These paths are dependent on each ion's initial trajectory, how they loose kinetic energy, their charge-state evolution, and their interaction with the coil generated magnetic field. A plot of output data for a typical Deflector simulation is shown in Fig. 2. In the sections that follow, we detail some key aspects of the Deflector code and how it determines the manner in which ions will stream from the target and be deflected from impacting final optics.

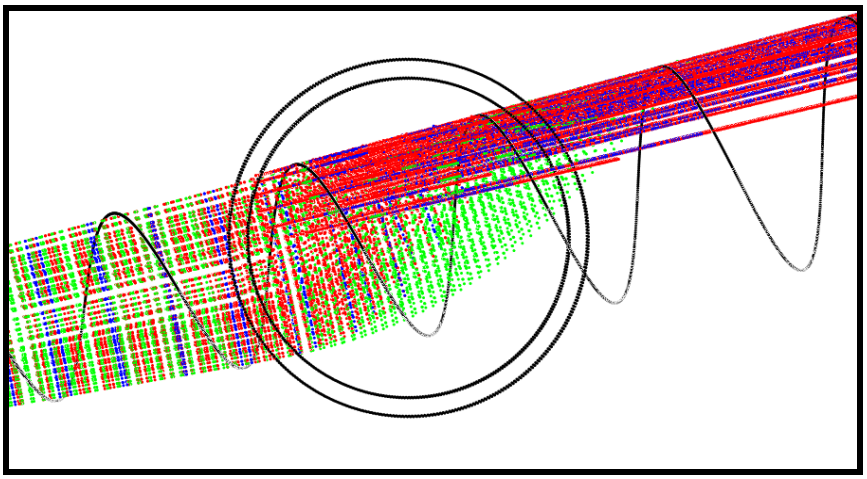

Fig. 2. A visualization of some components of Deflector's output data. Each point shows the stopping position of a simulation ion. Different shades represent the different ion species. The helical coil shows the beam tube wall and the concentric circles the magnet location.

II.A. Charge-State and Stopping-Power Assumptions

For ions penetrating thick or solid density targets an examination of the charge exchange (ionization and recombination) reaction rates shows that the time scale over which the ions reach an equilibrium charge-state is essentially instantaneous when compared to that for their stopping.[12] This allows treatment of the two processes to be decoupled by assuming a stopping-power (an ion's loss of energy per unit length of penetration) based on an equilibrium charge-state that is a function of an ion's instantaneous velocity.

However, in transiting rarefied gas targets (such as the low density xenon that might be present in a laser IFE target chamber) ionization and recombination processes can occur on timescales comparable to those of stopping processes. A detailed treatment of the ion-plasma interactions that determine slowing and charge-state evolution would involve difficult and historically unreliable discrete reaction calculations which have often been in gross error when compared to experiment. Fortunately, resorting to such complicated and error prone calculations was not necessary when writing Deflector's ion transport algorithms.

Because the task is to deflect ions away from final optics with magnetic fields or have them stop in the background gas, any algorithm we choose that underestimates both the charge states ions will achieve and the energy loss rates they will experience will be conservative. This is because we would predict less ion interaction with the magnetic fields (via $\mathbf{F} = q\mathbf{V}\times\mathbf{B}$ forces) and less slowing in the background gas, both of which would make it easier for ions to reach the final optics.

In reality the ions emerge from the target highly stripped. Since stopping is enhanced at charge states higher than equilibrium it is conservative to assume that the ions will always be in an equilibrium charge state. Further, it is conservative to assume that the ions transport through cold (non-ionized) background gas as stopping processes are enhanced by plasmas.[13] These approximations ensure that a particular ion deflection configuration would actually perform better than Deflector would predict.

To determine the slowing characteristics for each simulation ion at each point in time Deflector interpolates data contained in stopping-power tables generated with SRIM.[14] These calculations are independent of Deflector's determination of an equilibrium charge state value using Eq. (1); an expression proposed by Bohr, Betz, Brown, and Moak where Q_E is the equilibrium charge state, Z the ion's atomic number, v its speed, α the fine structure constant, and c the speed of light.[15]

$$Q_E = Z\cdot\left(1 - e^{\frac{-v}{Z^{\frac{2}{3}}\cdot\alpha\cdot c}}\right) \qquad (1)$$

II.B. Magnetic Field Calculations

The magnetic field profiles used by Deflector were generated via direct integration of the Biot-Savart equation for coil pairs in Helmholtz and non-Helmholtz configurations. At every point along a simulation ion's path, the magnetic force it will experience due to this field is determined. Within Deflector field profiles can be

scaled in both dimension and strength and their position modified in order to find an optimal configuration.

II.B. Plasma E and B Fields

Deflector employs an independent particle model and transports an appropriate simulation ion along a variable number of initial trajectories for each energy group of the user supplied target ion spectra. In reality, all the ions will be traversing the chamber concurrently and this calculation methodology neglects the possibility of their being significant plasma generated electric and magnetic fields to counter the external magnetic field imposed by the coil pair. Three-dimensional simulations were run with the particle-in-cell code LSP and showed no external magnetic field distortions with plasma fields on the order of 10^{-6} T. This is due primarily to the relatively low ion current densities that would be seen at the deflection magnet positions approximately 13 m from chamber center.[16]

II.D. Ion Charge-State Distributions

While it may be true that assuming an equilibrium charge state for a simulation ion is conservative in that the actual average charge state for the countless physical ions it represents will be greater, this treatment ignores the fact that those ions will display a charge state distribution about that mean. If the coefficient of variation for those distributions is large, a significant fraction of the physical ions could at any given time be less affected by an external magnetic field than the assumption of a single equilibrium charge state for their simulation ion would indicate.

For the lighter ions ($^{1, 2, 3}$H, $^{3, 4}$He) only a few possible ionization states exist with neutrality a small number of electron captures away from any attainable equilibrium or maximum ionization state. This makes the possibility of a significant neutral fraction at least qualitatively likely when compared to that for heavier ions expected to experience higher equilibrium charge states. To estimate the likelihood of this occurring, the code CHARGE (a component of LISE++) was used to determine the neutral fraction distributions and ionization cross sections for both hydrogen and helium across their energy spectra after passing through xenon target of thicknesses 7×10^{-4} kg/m^2 (10 m of xenon at 0.01 Torr and 300 K).[17] These neutral fractions were on the order of 10^{-5} - 10^{-6}.

Even these small fractions drastically overestimate the threat of neutrals, though. An examination of the ionization cross sections shows that the mean free path for such reactions for a 1 MeV ^{4}He ion, for example, is only ≈ 7 μm in xenon at 0.01 Torr and 300 K. This means that while at any given time one in 10^5 of these ions may be neutral, that will not be the case over any significant propagation distance and all light ions will be deflected by the magnetic field as if they were constantly at the equilibrium charge value.

Expected equilibrium ionization states for the heavy palladium and gold ions will be between 4^+ and 8^+. Charge state distribution widths show great regularity and can be estimated by the Eq. (2) where Z is the ion's atomic number and d_1 and w have been determined to be 0.32 and 0.45, respectively, for ions passing through argon and have been assumed the same for xenon.[18] This formula predicts an ionization distribution width of 1.8 e^- for Pd and 2.3 e^- for Au. A simple subtraction of half these values from their expected equilibrium charge states shows there is little risk of a significant neutral fraction. However, carbon ions ($^{12, 13}$C, the last ion species) will experience equilibrium charge states closer to neutrality. Once again, though, even if a significant neutral fraction were to be expected, the ionization cross section for a 1 MeV carbon shows that any individual ion would not remain neutral for more than ≈ 4 mm and the assumption taken by Deflector that all ions are constantly at the equilibrium value is again justified.

$$d = d_1 \cdot Z^w \qquad (2)$$

III. ION TRANSPORT RESULTS

Transient temperature analyses for the baseline HAPL program assumption of a tungsten armored first wall at the lowered xenon background gas pressures show that the target chamber will need a radius greater than 10 m to avoid significant damage.[19] For this work we have assumed the coil pairs will be placed 13 m from chamber center and the final optics have been granted a nominal target standoff distance of 26 m. Therefore, the deflected ions have approximately 13 m of beam tube wall over which they can impact before becoming a direct threat. The beam tube wall is modeled (as shown in Fig. 1) as right circular cone expanding from the target ignition point with some given divergence half-angle. The final optic position is treated simply as a critical plane normal to rays coming from chamber center, though, in reality they will be inclined quite a bit (85°) in the case of GIMMs. Our treatment of their placement when determining if ions reach them is therefore conservative.

While both types of optics will be located the same distance from chamber center, their orientation characteristics, the number of optics required, the type of driver used and uncertainty about laser fluence limits results in varying beam tube half-angles. Moreover, depending upon what type of laser is used (KrF or DPSSL) more or less drive energy is needed. Table I.

summarizes the base-cases for which coil sizes were determined to result in configurations providing a reduction in number of ions reaching the final optics by a factor of approximately 10^4. The details of two of the configurations are outlined below and Tables I and II give the pertinent simulation details and results for all configurations.

III.A. Case 1

This case assumes a GIMM final optic with its center located 26 m from the target. To accommodate a required KrF drive energy of 2.46 MJ across 60 beam-lines and a GIMM laser fluence limit of 5×10^4 J/m^2 necessitates a beam-tube half-angle of 1.13° (assuming right circular conical tubes). The target yield is 365 MJ.[20] Supplying Deflector with these parameters along with a center-of-coil-pair (COCP) magnetic field strength of 7.5×10^{-2} T and a profile consistent with a Helmholtz configuration for 1.0 m diameter coils yields a reduction in ion number-fluence (#/m^2) to the final optics by a factor of 4.8×10^4 and energy fluence (J/m^2) by a factor of 1.4×10^3.

III.B. Case 3

This case assumes a Fresnel final optic also positioned 26 m from the target. To accommodate a required DPSSL drive energy of 3.02 MJ across 48 final optics and a laser fluence limit of 2×10^4 J/m^2 necessitates a beam-tube half-angle of 2.21°. The target yield is 383 MJ. These parameters along with a COCP field strength of 7.5×10^{-2} T from a 1.8 m diameter coil pair result in a reduction in number-fluence by a factor of 2.0×10^4 and energy fluence by a factor of 6.3×10^2.

TABLE I. Evaluated cases for ion deflection concept.

Case	Optic Type	Driver	Fluence Limit (J/m^2)	Tube Half-Angle
1	GIMM	KrF	5×10^4 ($\perp$ to beam)	1.13°
2	GIMM	DPSSL	5×10^4 ($\perp$ to beam)	1.25°
3	Fresnel	DPSSL	2×10^4	2.21°
4	Fresnel	DPSSL	4×10^4	1.56°
5	Fresnel	DPSSL	6×10^4	1.27°

TABLE II. Summary of Deflector results for cases in Table I.

Case	Coil Diameter (m)	COCP Field Strength (T)	At Coil Field Strength (T)	# Fluence Reduction (N_0/N)	Energy Fluence Reduction (E_0/E)
1	1.0	7.5×10^{-2}	1.8×10^{-1}	4.8×10^4	1.4×10^3
2	1.0	7.5×10^{-2}	1.8×10^{-1}	1.4×10^4	4.3×10^2
3	1.8	7.5×10^{-2}	2.3×10^{-1}	2.0×10^4	6.3×10^2
4	1.3	7.5×10^{-2}	2.0×10^{-1}	2.5×10^4	7.7×10^2
5	1.0	7.5×10^{-2}	1.8×10^{-1}	1.2×10^4	3.8×10^2

IV. THE SPUTTERING THREAT

The possibility that successfully deflected ions impacting beam tube walls could generate potentially life-limiting final optic contamination warranted further investigation. To quantify this threat, ion impact angles, positions, and energies were tabulated with Deflector and combined with SRIM generated "sputtering yield" tables to estimate sputtering product characteristics and determine an upper bound on how much might reach the final optics. Fig. 3 shows the impact angle distribution helium ions in Case 5.

For each ion species SRIM was used to generate tables characterizing the sputtering products expected from impacts with a tungsten beam-tube as a function of impact angle and energy. These tables were combined with Deflector results detailing the location, frequency, and angle distribution of ion impacts to determine an upper limit on the amount of sputtering products that could potentially reach the final optics. Gold ions dominated this threat and we determined it they could deliver a maximum of 3×10^{12} tungsten atoms to the final optics. It is not known if this would be a significant amount over the lifetime of a final optic, but the beam tubes could certainly be engineered to limit sputtering by making grazing incidence impacts less likely.

V. SYSTEM POWER REQUIREMENTS

The power requirements for a system of 48 or 60 coil pairs to protect Fresnel or GIMM final optics, respectively, can be estimated fairly easily.[21] Assuming a copper resistivity of 1.7×10^{-8} Ω×m, a current density limit of 5×10^6 A/m^2, and the field strengths given in Table II, the power requirements for the evaluated deflection systems range from 2 – 6 MW.[22]

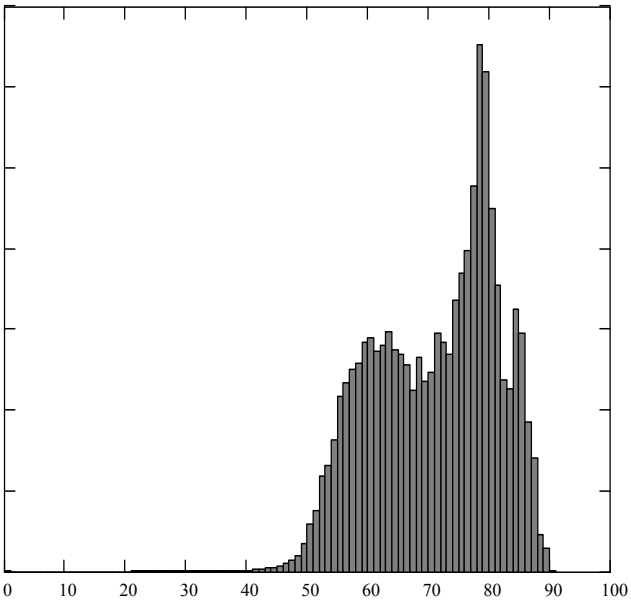

Fig. 3. Impact angle (0° is normal incidence) distribution for He ions deflected into the beam-tube walls.

VI. FURTHER WORK

Though we believe all the major feasibility issues of a magnetic deflection system to protect final optics have been addressed in the current body of research, there are several areas where further investigation would be valuable in increasing confidence in such systems. One potentially critical area where further efforts need to be focused is that of neutron shielding. The resistivity of copper has been observed to increase under fast neutron fluences which would lead to decreased magnetic deflection effectiveness as less current would flow through the coils and weaker field strengths would be generated.[23]

Beam tube heating and long term breakdown from deflected ion irradiation is also an area of concern. The coupling of Deflector results to a transient heat transfer code capable of treating penetrating radiation would show if there are any issues with excessive thermal loading on the beam tube walls in regions where the magnetic fields concentrate a large number of threat ions (just past the coil region in Fig. 2, for example). Ion irradiations of tungsten on accelerators with the threat ion species to IFE relevant fluences based on Deflector results would be useful in characterizing a beam tube's medium and long term response to the impact of deflected ions.

While the cases selected for analysis in this research reduce the ion threat substantially, it is likely that more optimized coil positions, magnetic field profiles, and beam tube geometries will lead to an even greater reduction in the threat to final optics. Automating Deflector for the purposes of conducting variation studies on these and other parameters may reveal more economic and effective ion deflection system configurations.

VII. CONCLUSIONS

Calculations have shown that excessive heating due to xenon condensation on targets during injection requires pressures of this protective background gas to be substantially lower than was previously assumed. Under these conditions, target output ions have been shown to be a significant life limiting hazard to final optics in a laser driven IFE power plant even when located several tens of meters from the ignition point.

This analysis of a simple magnetic deflection scheme shows that target generated ions can be successfully perturbed from trajectories that would otherwise lead to rapid or even single-shot failure of final optics. By using modest magnetic fields generated with normally conducing coil pairs, greater than 99.99 % of the ions that would otherwise threaten the final optics can be deflected into the laser beam tube walls.

The threat from sputtered atoms coming from ion impact sites on the beam tube walls has been quantified and bounded, though further analysis remains to determine if it is a credible secondary threat to the final optics. The power requirements for a full system of deflecting coils to protect all final optics would modest. The deflection coils may require substantial neutron shielding to protect the electrical properties of the conducting material but this issue has not been addressed.

ACKNOWLEDGMENTS

The authors would like to thank Dave Rose and the rest of the HAPL team for their invaluable input into this research.

This work was performed under the auspices of the U.S. Department of Energy by the University of California, Lawrence Livermore National Laboratory under contract No. W-7405-ENG-48.

REFERENCES

1. S. YU et al., "An Updated Point Design for Heavy Ion Fusion," *Fusion Sci. and Technol.*, **44**, 266 (2003).
2. W.R. Meier, "Osiris and SOMBRERO inertial fusion power plant designs–summary, conclusions, and recommendations," *Fusion Eng. and Design,* **25**, 145 (1994).

3. G. E. Rochau et al., "Progress Toward Development of an IFE Power Plant Using Z-Pinch Technology," *Fusion Sci. and Technol.*, **47**, 641 (2005).
4. W. R. Meier et al., "OSIRIS and SOMBRERO inertial fusion power plant designs. Final report. Volume 2. Designs, assessments, and comparisons," Report #: WJSA-92-01 DOE/ER/54100-1-VOL-2, p. 3-2, (1992).
5. C. Bibeau et al., "Full System Operations of Mercury: A Diode Pumped Solid-State Laser," *Fusion Science and Technology*, **47**, 581 (2005).
6. J.F. Latkowski et al., "Fused Silica Final Optics for Inertial Fusion Energy: Radiation Studies and System-Level Analysis," *Fusion sci. and Technol.*, **43**, 540 (2003).
7. W. R. Meier et al., "OSIRIS and SOMBRERO inertial fusion power plant designs. Final report. Volume 2. Designs, assessments, and comparisons," Report #: WJSA-92-01 DOE/ER/54100-1-VOL-2, p. 3-6, (1992).
8. Ibid., p. 4-41 to 4-47.
9. A.R. Raffray, "Target Thermo-Mechanical Modeling and Analysis," presented at the 7th High Average Power Laser Program Workshop, 2003, Retrieved December 7, 2005, from http://aries.ucsd.edu/HAPL/MEETINGS/0309-HAPL/raffraytarget.ppt#402,1, Slide 1
10. S. Furun et. al., "Dynamic Behavior of Bubbles and Blisters in Aluminum During Helium Ion Irradiation in an Electron Microscope," *Journal of Nuc. Mat.*, **155-157 prt 2**, p. 1149-1153.
11. R. P. Abbott, "Ion Deflection for Final Optics in Laser Fusion Power Plants," Viewgraphs, UCRL-PRES-217755.
12. M. S. Armel, "Atomic Processes for Heavy Ion Inertial Fusion," Ph.D. dissertation, University of California, Berkeley, CA, USA, 2000, p. 93.
13. E. Nardi and Z. Zinamon, "Charge State and Slowing of Fast Ions in Plasma," *Physical Review Letters*, **49**, 1251, (1982).
14. http://www.srim.org/
15. M. S. Armel, "Atomic Processes for Heavy Ion Inertial Fusion," Ph.D. dissertation, University of California, Berkeley, CA, USA, 2000, p. 96.
16. D. Rose, Personal Communications, (2005).
17. "Simulation of Fragment Separators," Retrieved December 8, 2005, from http://groups.nscl.msu.edu/lise/lise.html
18. H. D. Betz, "Charge States and Charge-Changing Cross Sections of Fast Heavy Ions Penetrating Through Gaseous and Solid Media," *Reviews of Modern Physics*, **44**, 465, (1972).
19. A.R. Raffray, "Blanket Design for Large Chambers," presented at the 13th High Average Power Laser Program Workshop, 2005, Retrieved December 7, 2005, from http://aries.ucsd.edu/HAPL/MEETINGS/0511-HAPL/Tuesday/15.0Raffray.ppt
20. L.J. Perkins, "HAPL Reactor Targets: Baseline Specifications and Future Options," presented at the 13th High Average Power Laser Program Workshop, 2005, Retrieved December 7, 2005, from http://aries.ucsd.edu/HAPL/MEETINGS/0511-HAPL/Tuesday/05.0Perkins.ppt
21. E. Dennison, "Axial Field of a Real Helmholtz Coil Pair," Retrieved December 8, 2005, from http://www.netdenizen.com/emagnet/helmholtz/realhelmholtz.htm
22. "Microscopic View of Copper Wire," Retrieved December 8, 2005, from http://hyperphysics.phy-astr.gsu.edu/hbase/electric/ohmmic.html